Plant Science 238 (2015) 178–187

Contents lists available at ScienceDirect

Plant Science

journal homepage: www.elsevier.com/locate/plantsci

# Cellular and molecular aspects of quinoa leaf senescence

María Paula López-Fernández[a,b,1], Hernán Pablo Burrieza[a,b,1], Axel Joel Rizzo[b], Leandro Julián Martínez-Tosar[a], Sara Maldonado[a,b,*]

[a] IBBEA (Instituto de Biodiversidad y Biología Experimental y Aplicada), CONICET (Consejo Nacional de Investigaciones Científicas Técnicas). Argentina
[b] DBBE (Departamento de Biodiversidad y Biología Experimental), FCEN (Facultad de Ciencias Exactas y Naturales), UBA (Universidad de Buenos Aires), Int. Güiraldes 2160, Ciudad Universitaria, C1428EGA, Argentina

ARTICLE INFO

*Article history:*
Received 16 February 2015
Received in revised form 1 June 2015
Accepted 2 June 2015
Available online 12 June 2015

*Keywords:*
DNA fragmentation
Endoreduplication
Leaf senescence
Nucleases
Quinoa

ABSTRACT

During leaf senescence, degradation of chloroplasts precede to changes in nuclei and other cytoplasmic organelles, RuBisCO stability is progressively lost, grana lose their structure, plastidial DNA becomes distorted and degraded, the number of plastoglobuli increases and abundant senescence-associated vesicles containing electronically dense particles emerge from chloroplasts pouring their content into the central vacuole. This study examines quinoa leaf tissues during development and senescence using a range of well-established markers of programmed cell death (PCD), including: morphological changes in nuclei and chloroplasts, degradation of RuBisCO, changes in chlorophyll content, DNA degradation, variations in ploidy levels, and changes in nuclease profiles. TUNEL reaction and DNA electrophoresis demonstrated that DNA fragmentation in nuclei occurs at early senescence, which correlates with induction of specific nucleases. During senescence, metabolic activity is high and nuclei endoreduplicate, peaking at 4C. At this time, TEM images showed some healthy nuclei with condensed chromatin and nucleoli. We have found that DNA fragmentation, induction of senescence-associated nucleases and endoreduplication take place during leaf senescence. This provides a starting point for further research aiming to identify key genes involved in the senescence of quinoa leaves.

Published by Elsevier Ireland Ltd.

## 1. Introduction

Leaf senescence involves a coordinated action at the cellular, tissue, organ, and organism levels, controlled by age under the influence of other endogenous and environmental factors [1]. To date, the mechanisms of this coordinated action, the integration mechanisms of the various senescence-affecting signals involved, as well as the nature and control of leaf aging, are key issues that still need to be studied because they are crucial for practical applications such as impact on crop yield, fruit ripening and biomass production.

During leaf senescence, cells of the epidermis and mesophyll are metabolically active, undergoing rather orderly changes in cell structure, metabolism, and gene expression. Cell death occurring in leaf senescence can be considered a type of PCD. During this process, chlorophyll and macromolecules such as proteins, membrane lipids, and RNA are degraded for redistribution of their components into other organs. The major proportion of leaf proteins are located in chloroplasts, being Ribulose-1,5-bisphosphate carboxylase/oxygenase (RuBisCO) and chlorophyll-binding light-harvesting proteins the most abundant among them, with chloroplasts being the source of most of the organic nitrogen recovered from senescing leaves [2]. During senescence, the vacuole is thought to be a potential destination of proteins ultimately degraded, and mitochondria are required to maintain cell viability [3].

One of the basic features of PCD is the non-random internucleosomal fragmentation of nuclear DNA (DNA laddering) which occurs as a result of specific nuclease activation prior to condensation of nuclear chromatin [4–7]. Nucleases can also be classified as endo- or exo-nucleases according to their enzymatic properties and further as either $Zn^{2+}$- (type I) or $Ca^{2+}$- (type II) nucleases, according to the metal ion cofactors and the optimum pH required for their activation [8]. Among $Ca^{2+}$-dependent nucleases, some can also be activated by $Mg^{2+}$ [9], $Mn^{2+}$ [10], or $Co^{2+}$ [11].

Leaf senescence involves the action of specific nucleases associated with programmed cell death (PCD) [12]. These single-stranded specific nucleases degrade both RNA and single-stranded

* Corresponding author at: Corresponding author at: Facultad de Ciencias Exactas y Naturales, Universidad de Buenos Aires, Intendente Güiraldes 2160 (C1428EGA) Ciudad de Buenos Aires, Argentina. Tel.: +54 1145763300; fax: +54 1145763384.
*E-mail addresses:* saram@bg.fcen.uba.ar, saram.maldonado@gmail.com (S. Maldonado).
[1] These authors contributed equally to this work.

http://dx.doi.org/10.1016/j.plantsci.2015.06.003
0168-9452/Published by Elsevier Ireland Ltd.

DNA (ssDNA), and have been described in many different cell types from microorganisms to mammals [13]. However, knowledge of the details regarding their biological functions is still limited [8]. According to Sakamoto and Takami [8], there are only three endonucleases characterised as potentially involved in leaf senescence: BFN1 (*bif*unctional *n*uclease1), CAN1 and CAN2 (*ca*lcium-dependent *n*uclease1 and 2). Among the exonucleases, DPD1 (defective in pollen organelle DNA degradation1, name of the mutants) is also involved in leaf senescence, being the DNA of chloroplasts and mitochondria its major target of degradation [8]. Furthermore, DPD1 is the only example among nucleases in which DNA degradation has been confirmed *in vivo* [14–17]. However, DNA degradation and the action of these nucleases remain limited because nucleases have high affinity to ssDNA and RNA and are localised in specific cellular compartments (namely, mitochondria and chloroplasts), raising the possibility that they do not act specifically on genomic DNA degradation.

Endopolyploidy is a developmental process involving one or several rounds of nuclear DNA synthesis without cytokinesis [18,19]. Endopolyploidy is generally considered the most common way to increase nuclear DNA content in plants [18]. Variations of DNA content have been linked with differentiation of highly specialised cell types such as vascular elements [20] and cells of the embryo suspensor [21]. Endopolyploidy has also been considered to have a role in coordinating the gene expression process required for interaction of nuclear and organelle genomes [22]. In seed storage tissues, endopolyploidy has also been associated with the high metabolic rates required during starch accumulation. In fact, high levels of ploidy have been detected in maize starchy endosperm [20,23], quinoa perisperm [24] and cotyledonary tissues of common beans [25]. In quinoa perisperm and cereal endosperm, endopolyploidy is also associated with PCD [24]. To our knowledge, endopolyploidy has not been linked to senescence yet. According to Sakamoto and Takami [8], the onset and progression of leaf senescence differ among plant species.

Quinoa (*Chenopodium quinoa* Willd.) is a grain crop from the Andes region of South America. This species has been cultivated for the last 7000 years and is well adapted to extreme environmental conditions such as high altitude, low annual precipitation, high soil salinity and freezing temperatures [26]. Quinoa is valued for its exceptional seed grain protein amino acid balance as well as for its high content of nutritionally favourable lipids [27–29]. The species belongs to the Amaranthaceae and is thus related to species such as beetroots, spinach and tumbleweeds. Similar to these species, quinoa leaves are eaten as a leaf vegetable. Preliminary observations in plants growing under controlled culture chambers have allowed us to detect differences in leaf longevity with regard to the quinoa genotype. Now, we addressed the analysis of senescence in the leaves of one of these genotypes, namely UDC9. This study examines leaf tissues during development and senescence using a range of well-established markers of PCD, by observation of: (i) morphological changes occurring in nuclei, vacuoles and chloroplasts, (ii) RuBisCO degradation, (iii) changes in chlorophyll content, (iv) DNA degradation, (v) changes in nuclease profiles, and (vi) increase in ploidy levels. This study is the preliminary stage of a larger project aiming to identify key genes involved in the multi-step process of senescence in quinoa leaves.

## 2. Material and methods

Quinoa (*Chenopodium quinoa* Willd.) cv. UDC9 plants were grown in a controlled chamber under 16-h light:8-h dark cycles at 25 °C. Materials were obtained from samples taken from the third and fourth leaves harvested at five different stages (Fig. 1A): *stage 1*, corresponding to a whitish leaf (as a result of the abundance of glandular hairs coating the blade surface), bearing a rough 10% of the final size; *stage 2*, corresponding to an intermediate stage between the white leaf stage and the mature green leaf stage; *stage 3*, corresponding to a full-sized mature leaf of bright green colour; *stage 4*, corresponding to a leaf starting to become yellowish; and *stage 5*, corresponding to a completely yellow leaf (Fig. 1A). In all experiments, the upper quarter regions of the leaf sheet were sampled. In all cases, leaves were sampled at noon.

### 2.1. Chlorophyll content evaluation

Relative chlorophyll content in leaves was determined non-destructively using a Minolta SPAD-502 chlorophyll-meter (Konica Minolta Sensing, Osaka, Japan) or in *N*,*N*-dimethylformamide extracts (10 mg fresh weight/4 ml) as described by Porra [30]. The average value of 12 measurements per leaf blade ($n$ = 3–5 leaf blades per treatment replicate, depending on the experiment) was used.

### 2.2. Sample preparation for light microscopy and transmission electron microscopy (TEM)

For histological analysis, immunogold and TUNEL assays, quinoa leaf sections were fixed for 4 h at 4 °C in 4% paraformaldehyde with 0.1 M phosphate buffered saline (PBS) (pH 7.2), dehydrated in a graded ethanol series (30%, 40%, 50%, 60%, 70%, 80%, 90%, 100%) and embedded in LRW resin (Polyscience Inc., Warrington, PA, USA; 17411) as previously described [31]. Semi-thin sections (1 μm thick) were mounted on glass slides and stained with 0.5% toluidine blue O (Sigma–Aldrich, St. Louis, MO, USA) in aqueous solution, or used without staining procedure.

For subcellular analysis, ultra-thin sections were fixed for 2 h at 4 °C using 2.5% glutaraldehyde in 0.1 M PBS, pH 7.2. Later they were post-fixed in 1% $OsO_4$ in the same buffer for 60 min, dehydrated in a graded ethanol series followed by an ethanol–acetone series and embedded in Spurr's resin (Sigma–Aldrich). Ultrathin sections were obtained with an ultramicrotome (Reichert-Jung, Vienna, Austria) using a diamond knife mounted on grids coated with Formvar (Polyscience Inc.), stained in uranyl acetate followed by lead citrate (EMS, Hatfield, PA, USA), and examined in a Zeiss M109 turbo (Zeiss, Wiesbaden, Germany) transmission electron microscope operating at an accelerating voltage of 90 kV.

### 2.3. Western blot analysis

Proteins extracts were obtained as follows: 100 mg of fresh leaf samples (Stages 1–5) were snap frozen in liquid nitrogen, immediately homogenized with mortar and pestle in 400 μl of extraction buffer (50 mM Tris–HCl pH7.4, 0.8% SDS, 5% β-mercaptoethanol, 10 mM NaCl, and Protease Inhibitor Cocktail), and chilled on ice for 30 min. The extracts were centrifuged for 10 min at 14,000 × *g*, 4 °C, and the supernatants were collected to eliminate tissue debris. This step was repeated until no pellets were observed. Protein concentration in the cleared extracts were determined as described by Bradford [32] using a Quick Start Bradford Protein Assay Kit 1 (BioRad 500–0201) with bovine serum albumin (BSA; Bio-Rad Laboratories, Hercules, CA, USA) as a standard. An aliquot of 10 μl of these protein extracts were loaded and fractionated on 12% acrilamide/*N*,*N*, bisacrilamide SDS-PAGE gels, using a Mini-Protean II apparatus (Bio-Rad Laboratories) and then electro-transferred onto a nitrocellulose membrane (Hybond Amersham Pharmacia Biotech, Freiburg, Germany) at 100 V for 1 h using a Mini Trans-Blot electrophoretic transfer cell (Bio-Rad Laboratories). An analytic SDS-PAGE run was performed separately to ensure equal protein loading by Coomasie Brilliant Blue staining (0.1% Coomassie R250, 10% acetic acid, 40% methanol) for 1 h at room temperature, and destained by several rinses with hot distilled water until proper contrast was achieved. Additionally, transferred membranes were

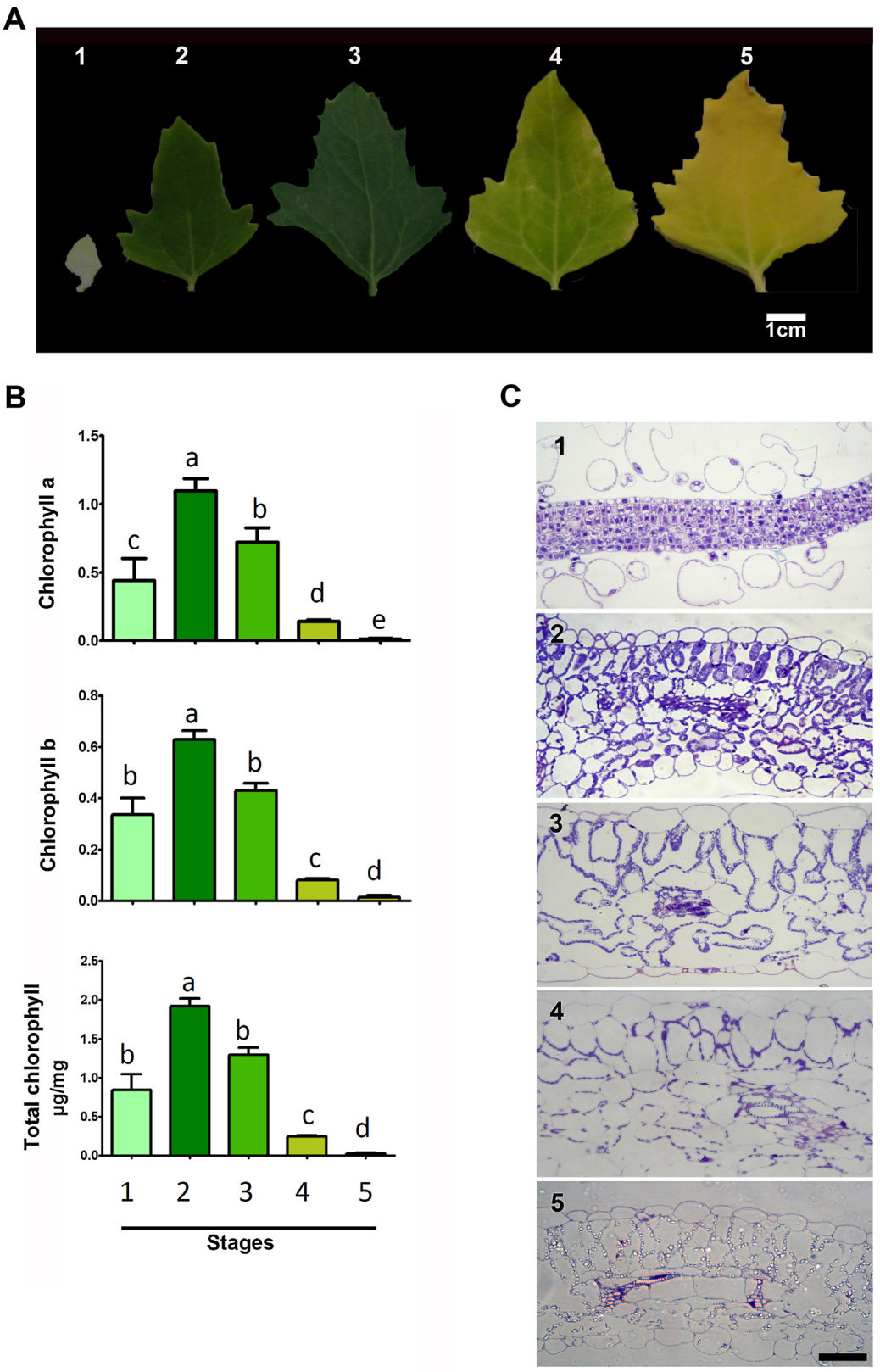


**Fig. 1.** (A–C) Quinoa leaves throughout development and senescence. (A) Stages 1–2 correspond to leaves growing in size, and changing colour during the maturation process; stage 3 corresponds to mature leaves; stages 4–5 correspond to leaves progressively senescing. (B) Quantitative changes in chlorophyll a, chlorophyll b and total chlorophyll during development and senescence. Each histogram is the mean ± standard deviation in three independent analyses. Different letters above the columns indicate significant differences (<0.05). (C) Leaf sections (LR White embedded sections, 1 μm thick) from stages 1 to 5. In each case, the figure is a representative result of observation of at least 10 whole-mounts of quinoa leaves at each stage. Bar: 50 μm.

stained with 0.1% (w/v) Ponceau S and 5% (v/v) acetic acid to check protein loading as well.

The membranes were immersed in blocking solution: 5% skimmed milk TBS (50 mM Tris–HCl, 150 mM NaCl, pH 8.0, 0.05% Tween-20) overnight at 4 °C, then incubated with a 1:4,000 dilution in blocking solution of a rabbit polyclonal anti-RuBisCO antiserum raised against RuBisCO's large subunit (kindly provided by J.J. Guiamet, Universidad Nacional de La Plata, Argentina) for 1 h on a bench top orbital shaker at room temperature. The membranes were then washed five times with TTBS (TBS, 0.05% Tween-20) at room temperature. Afterwards, each membrane was incubated with an alkaline phosphatase-conjugated goat anti-rabbit antibody (Jackson Immunoresearch 111-055-003, 1:5,000 dilution) for 1 h at room temperature, and then subjected to five 5-min rinses in TTBS solution. For the alkaline phosphatase-conjugated antibody, the membrane was incubated with 50 μl of a 2:1 NBT-BCIP (Promega) mixture in 10 ml of phosphatase buffer (100 mM Tris–HCl, pH 9,5; 100 nM NaCl; 5 mM $MgCl_2$) until deposition of the coloured product ensued.

### 2.4. In situ *immunolocalisation of RuBisCO*

Sections were first hydrated on a drop of Milli-Q-grade water for 5 min, rinsed in PBST (0.05% Tween 20 in 10 mM PBS, pH 7.4) and blocked for 90 min with 1% BSA in PBST at room temperature. The sections were then incubated overnight at 4 °C with rabbit anti-RuBisCO diluted 1:200 in PBST containing 0.1% BSA. Next, the sections were incubated for 1 h in a humid chamber with 5 nm diameter colloidal gold-conjugated goat antiserum raised to rabbit immunoglobulins diluted 1:200 in PBST plus 0.1% BSA. After 10 min fixation with 2.5% glutaraldehyde in 0.1 M PBS, pH 7.2, sections were thoroughly washed with Milli-Q-grade water. Finally, the sections were treated with silver enhancer, and contrasted in 0.1% toluidine blue O (Sigma–Aldrich) in aqueous solution.

Control sections were treated as above excluding the rabbit anti-RuBisCO antiserum.

### 2.5. *TUNEL assay*

The TUNEL assay evaluates the DNA integrity based on the ability of TdT (terminal deoxynucleotidyl transferase) to label blunt ends of double-stranded DNA (dsDNA) breaks allowing the localization of *in situ* DNA fragmentation.

DNA fragmentation was detected by terminal deoxynucleotidyltransferase-mediated dUTP-biotin nick end labeling (TUNEL) using the *In situ* Cell Death Detection Kit, Fluorescein (Roche). Cross-sections were obtained as described above. TUNEL labeling was performed according to the manufacturer's instructions. A negative control was included in each experiment by omitting TdT from the reaction mixture. As a positive control, permeabilised sections were incubated with DNase I (3 U/ml) for 15 min before the TUNEL assay. Counterstaining was done with 0.02 mg $ml^{-1}$ 4′-6-dianidino-2-phenylindole (DAPI) staining. The sections were mounted using the Citifluor™ mounting media (EMS).

Control treatments were conducted for each set of slides. Nuclei of leaves at stage 2 and 3, which act as an internal negative control, were not TUNEL-positive. TUNEL labeling was absent when Terminal deoxynucleotide Transferase (TdT) was omitted (data not shown). In positive controls previously treated with DNase, all the nuclei were labeled, thus validating the procedure.

Images for histological analysis and TUNEL were obtained by light microscopy and epifluorescence with an Axioskope 2 microscope (Carl Zeiss, Jena, Germany). The following filters were used to examine the fluorescent samples: DAPI filter (excitation 340–390 nm, emission 420–470 nm) and fluorescein filter (excitation 494–552 nm, emission 520–640 nm). Images were captured with a Cannon EOS 1000 D camera (Tokyo, Japan) and analysed using the AxioVision 4.8.2 software package (Carl Zeiss).

### 2.6. *DNA isolation and analysis*

Genomic DNA was isolated from 100 mg fresh leaves of the five stages using the DNeasy plant mini kit (Qiagen, Germany). Yield and quality of the DNA obtained were assessed in a NanoDrop spectrophotometer (Thermo Scientific NanoDrop 2000c). A 1.5 μg aliquot of DNA from each stage was separated on a 1% (w/v) agarose gel, and stained with ethidium bromide (final concentration: 0.5 μg/ml). A 1 kb Plus DNA Ladder (New England Biolabs, USA) was used as a reference.

### 2.7. *In-gel nuclease activity assay*

DNase activity was detected according to the method defined by Thelen and Northcote [33] with slight modifications. The samples were ground in liquid nitrogen and homogenised in extraction buffer (10 mM Tris–HCl pH 8.0, 1 mM EDTA, 20% glycerol, 0.1% SDS, 0.1 PMSF, 1 mM dithiothreitol (DTT). The cell extracts were centrifuged for 15 min at 14,000 × *g*, 4 °C, and the supernatant used for the assay. The protein concentrations were determined as described by Bradford [32] using a Quick Start Bradford Protein Assay Kit 1 (BioRad Laboratories 500–0201). Protein extracts were fractionated on SDS-PAGE gels containing 0.3 mg $ml^{-1}$ herring sperm DNA at 4 °C and 20 mA/plate. For single-stranded DNase activity, DNA was boiled for 5 min immediately prior to pouring the resolving gel. Equal amounts of protein (40 μg) were incubated for 10 min at 45 °C in buffer (0.125 M Tris pH 6.8, 10% [v/v] glycerol, 2% [w/v] SDS, 0.01% [w/v] bromophenol blue). As previously reported by Lesniewicz et al. [34], with modifications, after electrophoresis the gels were soaked in a buffer containing 25% 2-propanol and 1 mM EDTA for 15 min to remove SDS and residual divalent cations, and rinsed twice with water. Subsequently, the gels were washed twice for 5 min and incubated overnight in 10 mM Tris–HCl neutral buffer (pH 8.0, containing 10 mM $MgCl_2$, 10 mM $CaCl_2$) at 37 °C. After incubations, the gels were washed for 5 min in cold stop buffer (10 mM Tris–HCl pH 8.0, 1 mM EDTA). The gels were stained with SYBR® Safe DNA Gel Stain (Invitrogen, Carlsbad, CA, USA) to reveal the position of the nucleases and photographed using G-Box GeneSnap software from Syngene. Band intensity was analysed using the Gel-Pro Analyzer Software (Media Cybernetics Inc.).

### 2.8. *Flow cytometry analysis*

Leaves from different stages of development were dissected and chopped with Otto I extraction buffer and the nuclei-containing suspension was passed through a 50-μm filter. Then, the nuclei were stained with two volumes of Otto II staining solution containing DAPI [35]. After gently shaking the solution, samples were analysed with a flow cytometer (CyFlowPloidyAnalyser, Partec). Single-parameter histograms display relative fluorescence (i.e.: relative amount of DNA per cell) on the *x*-axis and the relative number of cells (number of cell counts along a definite period of time) on the *y*-axis.

## 3. Results

### 3.1. *Morphological changes in quinoa leaves during development and senescence*

Fig. 1B shows the evolution of chlorophyll content (chlorophyll a, chlorophyll b and total chlorophyll) during growth (stages 1–2) until leaves reached their maximum development (stage 3) and

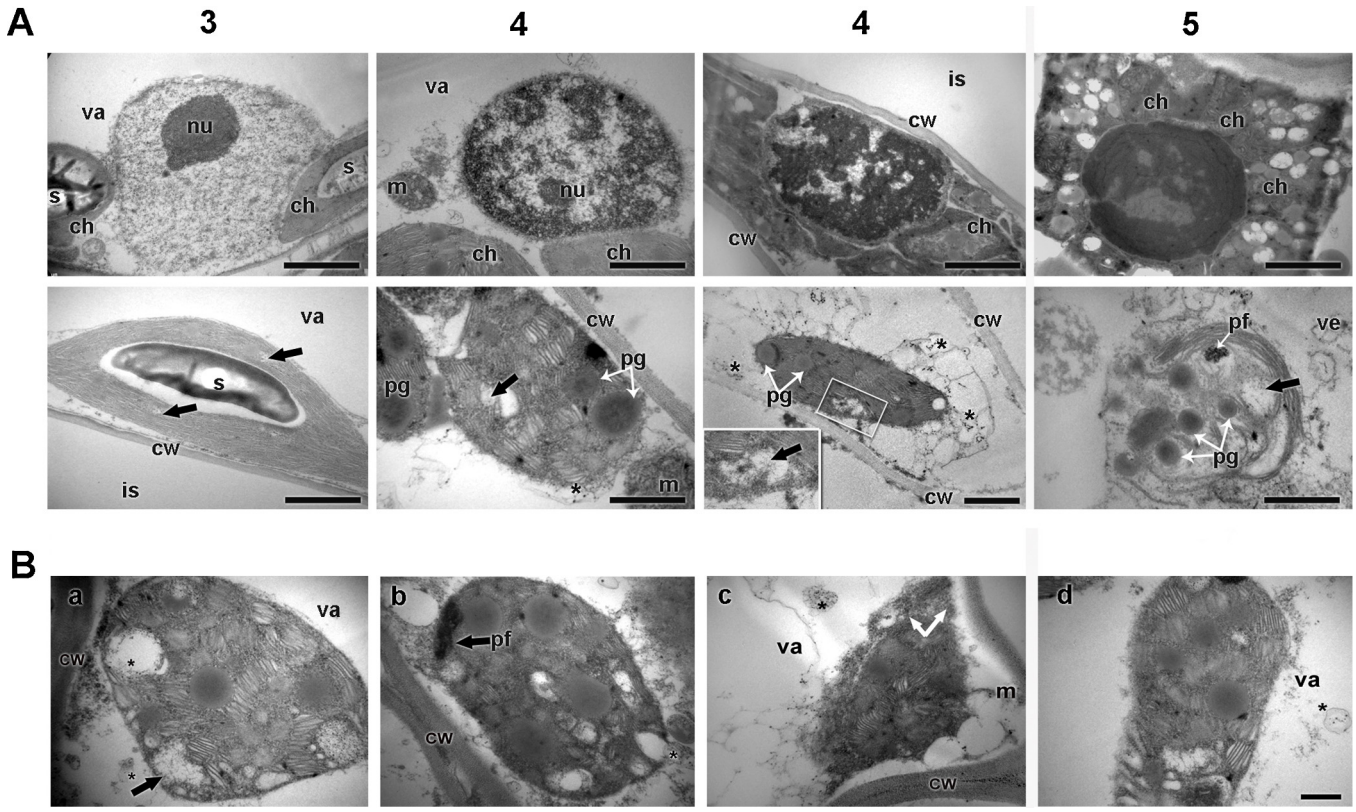


**Fig. 2.** (A). Nuclei (upper panel) and chloroplasts (lower panel) in mature (stage 3) and senescent leaves (stages 4 and 5). In each case, the figure is a representative result of the observation of ultrathin sections from five different leaves at each stage, using transmission electron microscopy. *Abbreviations*: ch, chloroplast; cw, cell wall; is, intercellular space; m, mitochondrion; nu, nucleolus; pf, phytoferritin, pb, plastoglobule s, starch; va, vacuole; ve, vesicle. Bars: 0.8 μm. Arrows indicate DNA areas in chloroplast; Asterisks indicates senescence-associated vesicles originated from chloroplasts. (B) Chloroplasts and senescence-associated vesicles (see asterisk) at stage 4, at four different situations: originating within the chloroplast, emerging from chloroplast and entering into the cytoplasm, within the cytoplasm, within the vacuole. Bars: 0.4 μm.

later, during senescence (stages 4–5). The contents of chlorophyll a and b increased dramatically during development, peaking at stage 2. Accordingly, leaves at stage 2 presented a more intense green colour. Between stages 2 and 3, chlorophyll a and b contents gradually decreased, being significantly lower in mature leaves (stage 3). Differences between stages 2 and 3 correspond to content of chlorophyll per unit fresh weight: at stage 2, cells were smaller and vacuoles more reduced, then the number of chloroplasts per unit area was higher.

Yellowing initiated near the tip of the leaf and gradually spread downwards (Fig. 1A). After 5–6 days, the whole leaf had turned yellow. The start and progression of leaf senescence was characterised by a dramatic decrease in chlorophyll content (stage 4), becoming negligible at stage 5.

Images of leaf cross-sections corresponding to the five stages studied are shown in Figs. 1C and 2. At the youngest stage, which corresponds to the whitish leaf of Fig. 1A, only cells of the glandular trichomes were differentiated; in cells of the mesophyll, vacuoles were still small in size. During development, the tissues grew by cellular expansion, i.e., each cell formed a large central vacuole and the mesophyll tissues developed intercellular spaces (Fig. 1C). At the mature stage, the mesophyll reached its maximum thickness. At these stages, nuclei showed large nucleoli and uncondensed or dispersed chromatin (Fig. 2A, upper panel). During early senescence, nuclei maintained intact nuclear membrane and nucleoli, but during late senescence, nucleoli disappeared and chromatin progressively condensed in clumps inside the nucleoplasm (Fig. 2A, upper panel).

Senescence involved the depletion of cytoplasm accompanied by organelle degradation. Chloroplasts were the first organelles showing visible damage (Fig. 2A, lower panel). At stage 3, chloroplasts exhibited starch grains in their stroma but chloroplast degeneration initiated at stage 4 and this was accompanied by chlorophyll degradation as reported above. At stage 5, chloroplasts lacking chlorophyll appeared totally degraded (Fig. 2A, lower panel).

Unlike plastids, mitochondria were required functioning to maintain cell viability.

In chloroplasts, synthesis of starch was disrupted from the early stages of senescence, grana lost their structure and thylakoids appeared progressively distended and degraded (Fig. 2A, lower panel). The number and size of plastoglobuli increased and translucent DNA-containing areas expanded (Fig. 2A, lower panel).

Fig. 2B shows senescence-associated vesicles (see asterisks) at stage 4, at four different situations: originating within the chloroplast (a), emerging from chloroplast and entering into the cytoplasm (b), within the cytoplasm, (c) within the vacuole (d).

### 3.2. RuBisCO during senescence

RuBisCO accumulation was studied by both Western blot and *in situ* immunoanalysis on leaves at mature and senescent stages in order to analyse the changes undergone throughout senescence, using a rabbit polyclonal anti-RuBisCO antiserum raised against RuBisCO's large subunit (Fig. 3).

Western blot clearly showed the presence of two major bands with molecular weight of approximately 53 kDa (Fig. 3A). The accumulation of RuBisCO was elevated in stage 3, lower in stage 4 and absent in stage 5.

The *in situ* immunolocalizations showed a correlation between RuBisCO abundance (Fig. 3A and B) and plastidial integrity (Fig. 2A and D).

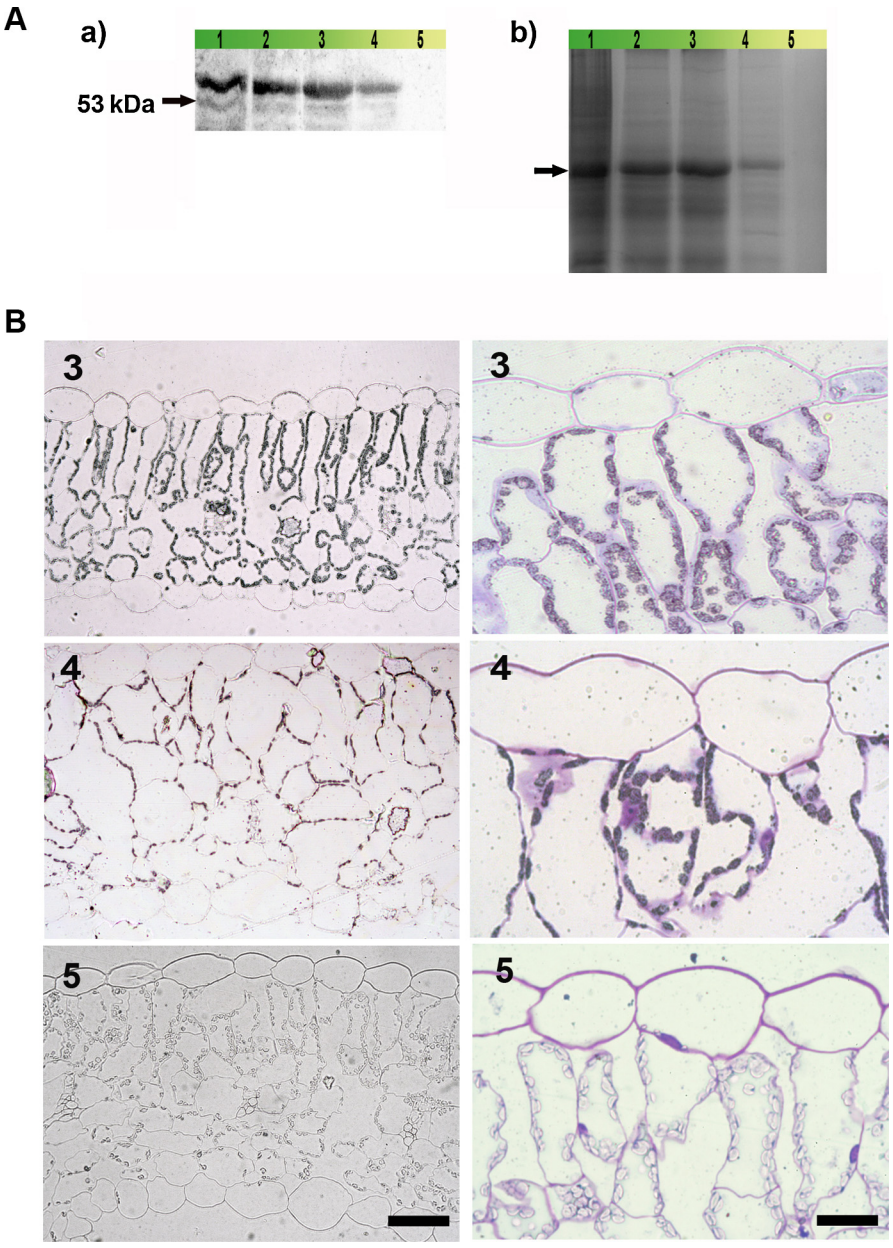


**Fig. 3.** RuBisCO was detected during senescence by Western blot (A) and *in situ* immunolocalization (B). Both analyses were carried out using a rabbit polyclonal RuBisCO antiserum raised against RuBisCO's large subunit. In A (a), protein samples (10 μl/lane) were separated on a 12% polyacrylamide gel and then transferred to a nitrocellulose membrane; (b), an analytic SDS-PAGE run was performed separately to ensure equal protein loading by Coomassie Brilliant Blue staining. In B, immunolocalization was carried out on semi-thin sections (1 μm thick); after immune treatment, sections were contrasted with toluidine blue O using two magnifications. Bars: 50 μm (right column); 15 μm (left column).

### 3.3. DNA fragmentation accompanies the progression of leaf senescence

DNA integrity was evaluated by agarose gel electrophoresis (Fig. 4A). At stages 4 and 5, (early and late senescence), as compared to stages 2 and 3, a smear was progresively visible (Fig. 4A). Some degree of DNA degradation was also visible at stage 1.

The fluorescein-dUTP-labeling assay detected nuclear DNA cleavage as a green fluorescent staining in the nuclei of cells under blue excitation. Fig. 4B shows representative TUNEL assay images in leaves at stages 1–5. DNA fragmentation was detected at stage 1 and at stages 4 and 5. DNA fragmentation, at stage 1, was attributed to the death of a few mesophyll cells. At the stages 2 and 3, labeling was totally absent (Fig. 4B). The first massive detectable events of DNA fragmentation began at stage 4 and continued until stage 5 (Fig. 4B).

### 3.4. Nuclease activities during development and senescence

Fig. 4C a and b shows DNA SDS-PAGE used to identify the activities of the DNases (a) and total protein content (b) during development and senescence. These enzymes encompass several classes of DNases based on their optimum pH and ion dependency. The patterns of $Ca^{2+}/Mg^{2+}$-dependent nucleases were different among stages as follows: (i) When dsDNA was used as substrate, at the stage 1, two bands with masses of 18 and 26 kDa were revealed; at the stage 2, only n26 was present; three bands with masses of 38, 33 and 26 kDa were revealed at stage 3; at stage 4 (early senescence) the activity of these bands increased notoriously, and an additional band of 18 kDa was clearly induced. Notably, the activity of n26 in this stage was about 30% higher than that of previous stages; at stage 5, the activity of n26 decreased, and the other three bands were barely detectable. (ii) When ssDNA was used as substrate at

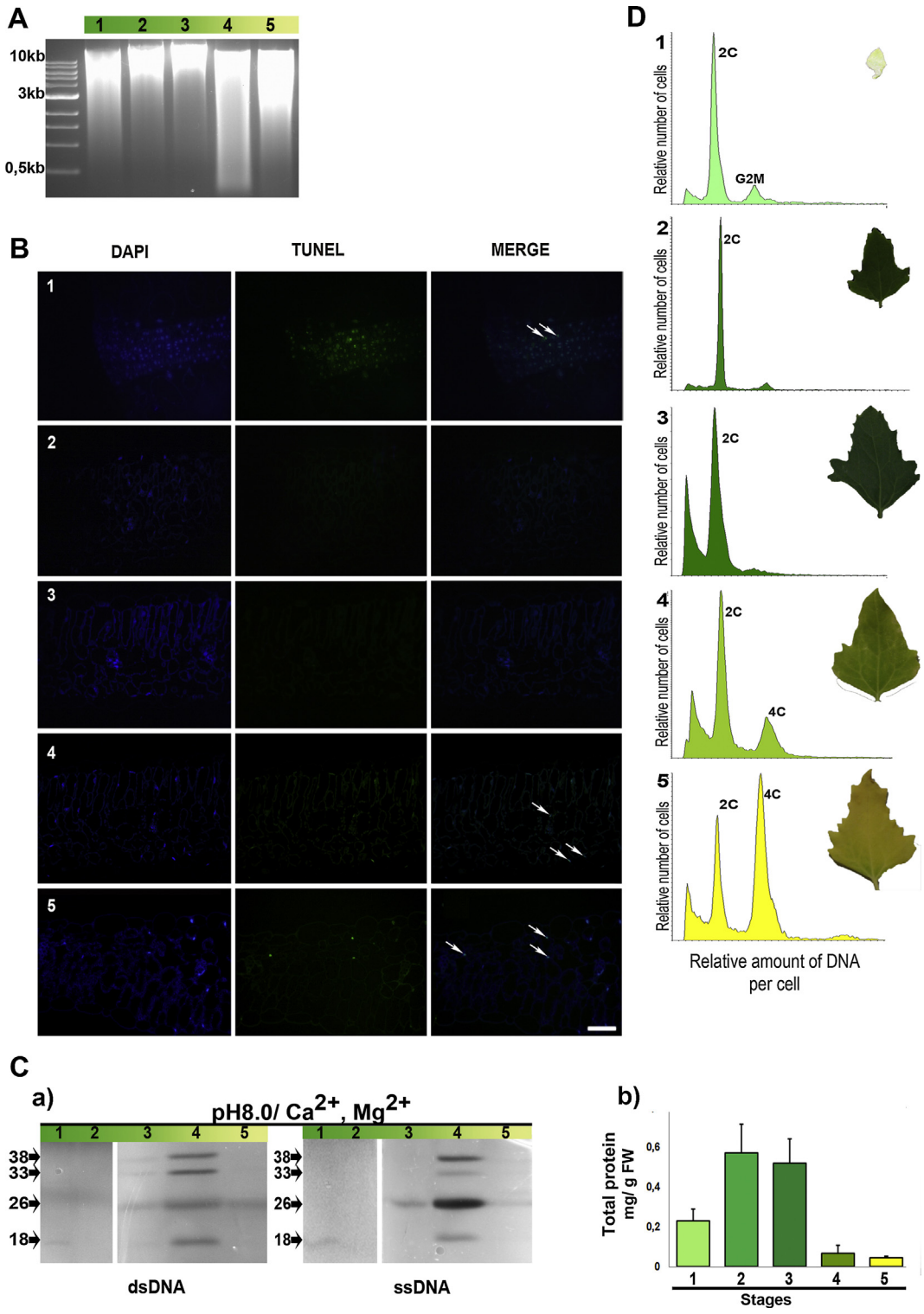


**Fig. 4.** DNA fragmentation (A and B), nucleases (C) and cytometry analysis (D) DNA fragmentation was analysed by gel electrophoresis (A) and TUNEL assay (B). For the TUNEL assay, semi-thin sections (1 μm thick) were stained with DAPI (left column) and TUNEL-labeled (right column). In each case, the figure is a representative result of the observation of at least five whole-mounts of quinoa leaves at each stage. For bright field images, see Fig. 1. Bars: 50 μm (A–D). Arrows indicate TUNEL-positive nuclei. (C) Identification of nucleases in quinoa leaves during development and senescence. (a) Protein samples (40 μg) extracted from mature or senescing leaves were resolved on an SDS-PAGE containing dsDNA and ssDNA as substrate. The gel was sliced, and the separate slices were incubated in buffer pH 8 supplemented with $Ca^{2+}$and $Mg^{2+}$; (b) Quantitative changes in total protein content during development and senescence. Each histogram is the mean ± standard deviation in three independent analyses. (D) Flow cytometric measurement of mean nuclear ploidy at different stages of quinoa leaf development and senescence. Histograms show the C-DNA levels at stages 1–5. The *x*-axis is the log of the fluorescence intensity: 2C peak corresponds to the diploid state of the genome; 4C peak indicates the tetraploid state of the genome (at stage 1, 4C indicates the capacity of the cells to enter in mitosis; at stage 4, 4C indicates endopoliploidy. The *y*-axis represents the cell counts (number of events per channel) per minute.

the same pH and ion conditions, no nuclease activity was detected at stage 2 and only one band of 18 kDa was detected at stage 1. The 26 kDa band was detected at stages 3 and 4, but its activity was 70% lower than that stage 4. At the onset of senescence (stage 4), the n26, n33 y n38 had the ability to digest both dsDNA and ssDNA but, its activity was different: n38 and n26 had higher activity in assays containing ssDNA as a substrate and n33 had higher activity in assays containing dsDNA. At stage 5, only one band with mass of 26 kDa was revealed in both assays, demonstrating no substrate specificity.

### 3.5. Changes in the ploidy, during development and senescence

Endoreduplication took place after the mature stage and continued during senescence. At this time, chromatin changed condensing in clumps.

Before stage 2, the C-numbers were 2 and 4 (Fig. 4D); 2C indicates the DNA level corresponding to the diploid state of the genome, whereas 4C indicates the ability of cells to enter M stage of the cell cycle or cells during actual mitosis. As development proceeded (stages 2 and 3), the number of 2C nuclei increased while the number of 4C nuclei decreased to disappear; this is because cell division had ceased at the late stage 2 and at stage 3 (Fig. 4D).

During senescence (stages 4 and 5), the DNA content was 2 and 4C. At these aging stages, 4C indicated endopolyploidy. As senescence further proceeded, the frequency of 2C nuclei decreased while the frequency of 4C nuclei progressively increased (Fig. 4D).

## 4. Discussion

Leaf senescence is an important and complex process in the plant life cycle, which is thought to contribute to fitness through the recycling of nutrients to actively growing regions [36]. Leaf senescence involves massive structural and functional disintegration of cells through the activation of various hydrolytic activities [37,38]. These hydrolytic activities are required to degrade the organic components that accumulate during the vegetative growth phase and, subsequently, to mobilize the degraded products. Degradation of proteins induced by senescence takes place within the plastids and may continue in cytoplasmic vesicles due to the presence of active cysteine proteases in the cytoplasm [39,40]. In quinoa, particularly during early senescence, we found that the vesicular transport system is very active. Subsequently, the chloroplast envelope membrane is disassembled before total disorganization of the thylakoids and total dissolution of plastoglobuli (Fig. 2D). In quinoa leaves, the simultaneous analysis of mesophyll cellsúltrastructure, chlorophyll concentration and RuBisCO integrity showed that the decrease in chlorophyll a and b, and the degradation of RuBisCO during senescence (Fig. 3) correlated with the gradual disintegration of thylakoid membranes, as well as with damages in chloroplastidial DNA (Fig. 2).

Nuclear DNA fragmentation has been reported in cells from foliar tissues during leaf senescence in different plant species [7,41]. In quinoa, we detected DNA fragmentation in leaf tissues by the TUNEL assay and genomic DNA electrophoresis. At early stages of quinoa leaf development, a few nuclei showed TUNEL-positive labeling while some degree of DNA smearing was evident in the electrophoretic run. This is most attributable to a normal PCD process needed to enlarge some intercellular spaces of the chlorenchyma in the mesophyll but the first massive detectable events of DNA fragmentation began *ab initio* of senescence, coincidently with the start of yellowing, and continued until the end of the leaf life cycle (Fig. 4B).

Another PCD hallmark in nuclei is chromatin condensation, which leads to DNA laddering into 180-bp nucleosomal units. However, if the proteins constituting the nucleosomes are degraded before or during the induction of nuclease activity, sharply defined nucleosomal DNA ladders may not form and the DNA degradation pattern will be more random [42]. In this study, we detected DNA smearing instead of DNA laddering (Fig. 4A).

Decreases in both chlorophyll and RuBisCO levels have been used as classical indicators of leaf senescence ([43]; for a review, see [44]). According to Nooden et al. [45], chloroplast breakdown is accompanied by degradation of protein complexes or damage to any of their components, which immediately triggers the whole degradation of the chloroplast's ultrastructure: swelling and breakage of thylakoids and an increase in the number and size of plastoglobuli, which correlate with chlorophyll degradation. Such changes are consistent with earlier data gathered during leaf senescence in *Phaseolus vulgaris* L. [46], *Prunus persica* Stokes [47], *Ornithogalum virens* L. and *Nicotiana tabacum* L. [7].

Wu et al. [48] identify four categories of genes, regulating the speed and transition of early leaf growth, photosynthesis rate, and the onset and progression of leaf senescence. During this highly regulated process, hydrolytic enzymes become activated to redistribute cell components; among them, specific nucleases are induced [11,49–52]. Nuclease activity is associated with nuclear DNA fragmentation phenomena [34,53]. Plant S1-like nucleases, the main class of single-stranded specific nucleases (often termed as type I nucleases), degrade both RNA and ssDNA during plant PCD [54]. Here, we observed that the activity of neutral nucleases with molecular masses of approximately 38, 33 and 26 kDa was induced at early senescent stages. BFN1 is a nuclease with a molecular mass of approximately 38 kDa which has been detected in *Arabidopsis* during leaf and stem senescence [54–56]. The specific function of BFN1 has not yet been demonstrated, but it has been suggested to be involved in the nucleic acid degradation that takes place during both senescence and developmental PCD [56]. In quinoa, we found some DNase activity in mature leaves but a marked strong DNase activity became readily apparent only during leaf senescence in accordance with the timing of induction of nuclease activity; similar to BFN1, the n38 in quinoa was induced at the onset of senescence.

DPD1 belongs to the family of exonucleases and it has been localized in both plastids and mitochondria. Tang and Sakamoto [57] find that the expression of DPD1 is high in senescing *Arabidopsis* leaves. This nuclease has a molecular mass of 32 kDa, and shows dsDNA preference [15]. In quinoa, a nuclease of around 33 kDa showed a clear preference towards dsDNA substrate at stage 4. We infer that the *Arabidopsis* DPD1 might correspond to n33 in quinoa.

Several authors consider the condensation of chromatin as one of the hallmarks of PCD [7,41,58,59]. During the onset of quinoa leaves' senescence, nuclei maintained intact nuclear membranes and nucleoli, and chromatin condensed partially in chromosomes inside the nucleoplasm. We associated the initial condensation of chromatin with the process of endoreduplication that takes place during senescence (Fig. 4D). At this time, chromatin did not appear agglutinated, and thus did not seem to be degraded.

Endoreduplication is a form of nuclear polyploidization that results in multiple uniform copies of chromosomes. This process is common in plants and animals, especially in tissues with high metabolic activity, and generally occurs in cells that are terminally differentiated. Recently Scholes and Paiges [21] suggest that plant endoreduplication is an adaptive, plastic response to mitigate the effects of stress. It is also thought that endoreduplication provides a mechanism to increase the level of gene expression. Plant endoreduplication is well documented in the endosperm and cotyledons of developing seeds, but also occurs in many tissues throughout the plant. Numerous observations have been made on endoreduplication, or at least on extra cycles of the S-phase, as

a consequence of mutations in genes controlling several aspects of cell cycle regulation. However, until recently, few studies had focused on the molecular mechanisms responsible for this specialised cell cycle phenomenon, and the overall functionality of this process demands further investigation. It has been suggested that endoreduplication requires nothing more elaborate than a loss of M-phase cyclin-dependent kinase activity and oscillations in the activity of S-phase cyclin-dependent kinase. Previously, endopolyploidy in quinoa had been associated with the synthesis of compound starch grains in storage seed tissues during PCD [24]. Also in quinoa, Kolano et al. [60] report that DNA contents ranging from 2C to 16C are found in different proportions in root, hypocotyl and cotyledons, but they also emphasize that endopolyploidy do not occur in leaves. Conversely, now we found that nuclei progressively endoreduplicated. The process started after stage 3 (mature stage) and increased throughout senescence. To our knowledge, there is no evidence so far which would support differential cell death events affecting 2C cells but not 4C cells, and thus, any reduction of the 2C/4C ratio should be taken as an indication of cells undergoing endoreduplication. Furthermore, DNA content in cells from tomato leaves increases during plant development from 2C in the very young seedling stage, to a mixture of cells with DNA amounts ranging from 2C to 128C at senescence [61]. This particular issue will be addressed by further investigation.

## Acknowledgments

This work was supported by the Universidad de Buenos Aires (UBACYT 20020100100232 to S.M.), the Consejo Nacional de Investigaciones Científicas y Técnicas (CONICET. Res. 810/13.PIP 0465 to SM) and the Fundación Juan Bautista Sauberan (to HB and SM).

## References

[1] P.O. Lim, H.J. Kim, H.G. Nam, Leaf senescence, Annu. Rev. Plant Biol. 58 (2007) 115–136, http://dx.doi.org/10.1146/annurev.arplant.57.032905.105316
[2] L. Avila-Ospina, M. Moison, K. Yoshimoto, C. Masclaux-Daubresse, Autophagy, plant senescence, and nutrient recycling, J. Exp. Bot. (2014), http://dx.doi.org/10.1093/jxb/eru039
[3] J. Dangl, R. Dietrich, H. Thomas, Senescence and programmed cell death, in: B. Buchanan, W. Gruissem, R. Jones (Eds.), Biochem. Mol. Biol. Plants, American Society of Plant Physiologists, Rockville, Maryland, 2000, pp. 1044–1100.
[4] J. Cao, F. Jiang, Sodmergen, K. Cui, Time-course of programmed cell death during leaf senescence in Eucommia ulmoides, J. Plant Res. 116 (2003) 7–12, http://dx.doi.org/10.1007/s10265-002-0063-5
[5] B. Uzelac, D. Janosević, S. Budimir, In situ detection of programmed cell death in *Nicotiana tabacum* leaves during senescence, J. Microsc. 230 (2008) 1–3, http://dx.doi.org/10.1111/j.1365-2818.2008.01947.x
[6] F. Domínguez, F.J. Cejudo, Programmed cell death (PCD): an essential process of cereal seed development and germination, Front. Plant Sci. 5 (2014) 1–11, http://dx.doi.org/10.3389/fpls.2014.00366
[7] E. Simeonova, A. Sikora, M. Charzyńska, A. Mostowska, Aspects of programmed cell death during leaf senescence of mono- and dicotyledonous plants, Protoplasma 214 (2000) 93–101, http://dx.doi.org/10.1007/BF02524266
[8] W. Sakamoto, T. Takami, Nucleases in higher plants and their possible involvement in DNA degradation during leaf senescence, J. Exp. Bot. (2014), http://dx.doi.org/10.1093/jxb/eru091
[9] F. Domínguez, F.J. Cejudo, Identification of a nuclear-localized nuclease from wheat cells undergoing programmed cell death that is able to trigger DNA fragmentation and apoptotic morphology on nuclei from human cells, Biochem. J. 397 (2006) 529–536, http://dx.doi.org/10.1042/BJ20051809
[10] X. He, A.R. Kermode, Proteases associated with programmed cell death of megagametophyte cells after germination of white spruce (*Picea glauca*) seeds, Plant Mol. Biol. 52 (2003) 729–744, http://www.ncbi.nlm.nih.gov/pubmed/13677463.
[11] B.J. Langston, S. Bai, M.L. Jones, Increases in DNA fragmentation and induction of a senescence-specific nuclease are delayed during corolla senescence in ethylene-insensitive (etr1-1) transgenic petunias, J. Exp. Bot. 56 (2005) 15–23, http://dx.doi.org/10.1093/jxb/eri002
[12] S. Farage-Barhom, S. Burd, L. Sonego, A. Mett, E. Belausov, D. Gidoni, et al., Localization of the Arabidopsis senescence- and cell death-associated BFN1 nuclease: from the ER to fragmented nuclei, Mol. Plant 4 (2011) 1062–1073, http://dx.doi.org/10.1093/mp/ssr045
[13] N.a. Desai, V. Shankar, Single-strand-specific nucleases, FEMS Microbiol. Rev. 26 (2003) 457–491, http://www.ncbi.nlm.nih.gov/pubmed/12586391.
[14] N. Nagata, C. Saito, A. Sakai, H. Kuroiwa, T. Kuroiwa, The selective increase or decrease of organellar DNA in generative cells just after pollen mitosis one controls cytoplasmic inheritance, Planta 209 (1999) 53–65, http://dx.doi.org/10.1007/s004250050606
[15] R. Matsushima, L.Y. Tang, L. Zhang, H. Yamada, D. Twell, W. Sakamoto, A conserved, $Mg^{2+}$-dependent exonuclease degrades organelle DNA during Arabidopsis pollen development, Plant Cell. 23 (2011) 1608–1624, http://dx.doi.org/10.1105/tpc.111.084012
[16] L.Y. Tang, R. Matsushima, W. Sakamoto, Mutations defective in ribonucleotide reductase activity interfere with pollen plastid DNA degradation mediated by DPD1 exonuclease, Plant J. 70 (2012) 637–649, http://dx.doi.org/10.1111/j.1365-313X.2012.04904.x
[17] D. Wang, Q. Zhang, Y. Liu, Z. Lin, S. Zhang, M.X. Sun, et al., The levels of male gametic mitochondrial DNA are highly regulated in angiosperms with regard to mitochondrial inheritance, Plant Cell. 22 (2010) 2402–2416, http://dx.doi.org/10.1105/tpc.109.071902
[18] F. D'Amato, Polyploidy in cell differentiation, Caryologia 42 (1989) 183–211, http://dx.doi.org/10.1080/00087114.1989.10796966
[19] J. Traas, M. Hülskamp, E. Gendreau, H. Höfte, Endoreduplication and development: rule without dividing? Curr. Opin. Plant Biol. 1 (1998) 498–503, http://www.ncbi.nlm.nih.gov/pubmed/10066638.
[20] B.a. Larkins, B.P. Dilkes, R.a. Dante, C.M. Coelho, Y.M. Woo, Y. Liu, Investigating the hows and whys of DNA endoreduplication, J. Exp. Bot. 52 (2001) 183–192, http://www.ncbi.nlm.nih.gov/pubmed/11283162.
[21] D.R. Scholes, K.N. Paige, Plasticity in ploidy: a generalized response to stress, Trends Plant Sci. (2014), http://dx.doi.org/10.1016/j.tplants.2014.11.007
[22] S.J. Cookson, A. Radziejwoski, C. Granier, Cell and leaf size plasticity in Arabidopsis: what is the role of endoreduplication? Plant Cell Environ. 29 (2006) 1273–1283, http://dx.doi.org/10.1111/j.1365-3040.2006.01506.x
[23] R.V. Kowles, F. Srienc, R.L. Phillips, Endoreduplication of nuclear DNA in the developing maize endosperm, Dev. Genet. 11 (1990) 125–132, http://dx.doi.org/10.1002/dvg.1020110202
[24] M.P. López-Fernández, S. Maldonado, Programmed cell death during quinoa perisperm development, J. Exp. Bot. 64 (2013) 3313–3325, http://dx.doi.org/10.1093/jxb/ert170
[25] R. Bino, Flow cytometric determination of nuclear replication stage in seed tissues, Ann. Bot. 72 (1993) 181–187, http://dx.doi.org/10.1006/anbo.1993.1097
[26] M. Tapia, Agrobiodiversidad en los Andes, Fundación Friedrich Ebert, Lima (1999).
[27] M.J. Kozioł, Chemical composition and nutritional evaluation of quinoa (*Chenopodium quinoa* Willd), J. Food Compos. Anal. 5 (1992) 35–68, http://dx.doi.org/10.1016/0889-1575(92)90006-6
[28] H.N. Oshodi, M.O. Ogungbenle, A.A. Oladi, Chemical composition, nutritionally valuable minerals and functional properties of benniseed (*Sesamum radiatum*), pearl millet (*Pennisetum typhoides*) and quinoa (*Chenopodium quinoa*) flours, Int. J. Food Sci. Nutr. 50 (1999) 325–331, http://dx.doi.org/10.1080/096374899101058
[29] M. Koziol, Quinoa: a potential new oil crop, in: J.E. Janick, J. Simon (Eds.), New Crop., Wiley, New York, 1993, pp. 328–336.
[30] R.J. Porra, The chequered history of the development and use of simultaneous equations for the accurate determination of chlorophylls a and b, Photosynth. Res. 73 (2002) 149–156, http://dx.doi.org/10.1023/A:1020470224740
[31] K.F. Harris, Z. Pesic-Van Esbroeck, J.E. Duffus, Moderate-temperature polymerization of LR White in a nitrogen atmosphere, Microsc. Res. Tech. 32 (1995) 264–265, http://dx.doi.org/10.1002/jemt.1070320312
[32] M.M. Bradford, A rapid and sensitive method for the quantitation of microgram quantities of protein utilizing the principle of protein-dye binding, Anal. Biochem. 72 (1976) 248–254, http://www.ncbi.nlm.nih.gov/pubmed/942051.
[33] M.P. Thelen, D.H. Northcote, Identification and purification of a nuclease from *Zinnia elegans* L.: a potential molecular marker for xylogenesis, Planta 179 (1989) 181–195, http://dx.doi.org/10.1007/BF00393688
[34] K. Leśniewicz, J. Pieńkowska, E. Poreba, Characterization of nucleases involved in seedling development of cauliflower, J. Plant Physiol. 167 (2010) 1093–1100, http://dx.doi.org/10.1016/j.jplph.2010.03.011
[35] F. Otto, DAPI staining of fixed cells for high-resolution flow cytometry of nuclear DNA, Methods Cell Biol. 33 (1990) 105–110, http://www.ncbi.nlm.nih.gov/pubmed/1707478.
[36] V. Buchanan-Wollaston, T. Page, E. Harrison, E. Breeze, O.L. Pyung, G.N. Hong, et al., Comparative transcriptome analysis reveals significant differences in gene expression and signalling pathways between developmental and dark/starvation-induced senescence in Arabidopsis, Plant J. 42 (2005) 567–585, http://dx.doi.org/10.1111/j.1365-313X.2005.02399.x
[37] L.D. Noodén, The phenomena of senescence and aging, in: L. Noodén, A. Leopold (Eds.), Senescence and Aging in Plants, Academic Press, San Diego, 1988, pp. 1–50.
[38] H.R. Woo, K.M. Chung, J.H. Park, S.A. Oh, T. Ahn, S.H. Hong, et al., ORE9, an F-box protein that regulates leaf senescence in Arabidopsis, Plant Cell. 13 (2001) 1779–1790, http://dx.doi.org/10.1105/TPC.010061
[39] C.A. Carrión, M.L. Costa, D.E. Martínez, C. Mohr, K. Humbeck, J.J. Guiamet, In vivo inhibition of cysteine proteases provides evidence for the involvement of "senescence-associated vacuoles" in chloroplast protein degradation during dark-induced senescence of tobacco leaves, J. Exp. Bot. 64 (2013) 4967–4980, http://dx.doi.org/10.1093/jxb/ert285
[40] M. Díaz-Mendoza, B. Velasco-Arroyo, P. González-Melendi, M. Martínez, I. Díaz, C1A cysteine protease–cystatin interactions in leaf senescence, J. Exp. Bot. 65 (2014) 3825–3833, http://dx.doi.org/10.1093/jxb/eru043

[41] C.H. Yen, C.H. Yang, Evidence for programmed cell death during leaf senescence in plants, Plant Cell Physiol. 39 (1998) 922–927, http://dx.doi.org/10.1093/oxfordjournals.pcp.a029455
[42] R. Mittler, E. Lam, Identification, characterization, and purification of a tobacco endonuclease activity induced upon hypersensitive response cell death, Plant Cell. 7 (1995) 1951–1962, http://dx.doi.org/10.1105/tpc.7.11.1951
[43] H. Thomas, C.M. Smart, Crops that stay green, Ann. Appl. Biol. 123 (1993) 193–219, http://dx.doi.org/10.1111/j.1744-7348.1993.tb04086.x
[44] J. Stoddart, H. Thomas, Leaf senescence, in: D. Boulter, B. Parthier (Eds.), Encycl. Plant Physiol, Springer-Verlag, Berlin, 1982, pp. 592–636.
[45] L.D. Nooden, Senescence mechanisms, Physiol. Plant 99 (1997) 511–753, http://dx.doi.org/10.1111/j.1399-3054.1997.tb01059.x
[46] R. Barton, Fine structure of mesophyll cells in senescing leaves of Phaseolus, Planta 71 (1966) 314–325, http://dx.doi.org/10.1007/BF00396319
[47] N. Nii, S. Kawano, S. Nakamura, T. Kuroiwa, Changes in the fine structure of chloroplast and chloroplast DNA of peach leaves during senescence, Engei Gakkai Zasshi. 57 (1988) 390–398, http://dx.doi.org/10.2503/jjshs.57.390
[48] X.-Y. Wu, B.-K. Kuai, J.-Z. Jia, H.-C. Jing, Regulation of leaf senescence and crop genetic improvement, J. Integr. Plant Biol. 54 (2012) 936–952, http://dx.doi.org/10.1111/jipb.12005
[49] A. Blank, T. McKeon, Single-strand-preferring nuclease activity in wheat leaves is increased in senescence and is negatively photoregulated, Proc. Natl. Acad. Sci. U.S.A. 86 (1989) 3169–3173.
[50] M. Wood, J.B. Power, M.R. Davey, K.C. Lowe, B.J. Mulligan, Factors affecting single strand-preferring nuclease activity during leaf aging and dark-induced senescence in barley (*Hordeum vulgare* l.), Plant Sci. 131 (1998) 149–159, http://dx.doi.org/10.1016/S0168-9452(97)00253-7
[51] A. Lers, E. Lomaniec, S. Burd, A. Khalchitski, The characterization of LeNUC1, a nuclease associated with leaf senescence of tomato, Physiol. Plant 112 (2001) 176–182, http://www.ncbi.nlm.nih.gov/pubmed/11454222.
[52] L. Canetti, E. Lomaniec, Y. Elkind, A. Lers, Nuclease activities associated with dark-induced and natural leaf senescence in parsley, Plant Sci. 163 (2002) 873–880, http://dx.doi.org/10.1016/S0168-9452(02)00242-X
[53] Y. Xu, M.R. Hanson, Programmed cell death during pollination-induced petal senescence in petunia, Plant Physiol. 122 (2000) 1323–1333, http://dx.doi.org/10.1104/pp.122.4.1323
[54] K. Lesniewicz, W.M. Karlowski, J.R. Pienkowska, P. Krzywkowski, E. Poreba, The plant s1-like nuclease family has evolved a highly diverse range of catalytic capabilities, Plant Cell Physiol. 54 (2013) 1064–1078, http://dx.doi.org/10.1093/pcp/pct061
[55] M. Pérez-Amador, M.L. Abler, E.J. De Rocher, D.M. Thompson, A. van Hoof, N.D. LeBrasseur, et al., Identification of BFN1, a bifunctional nuclease induced during leaf and stem senescence in Arabidopsis, Plant Physiol. 122 (2000) 169–180.
[56] S. Farage-Barhom, S. Burd, L. Sonego, R. Perl-Treves, A. Lers, Expression analysis of the BFN1 nuclease gene promoter during senescence, abscission, and programmed cell death-related processes, J. Exp. Bot. 59 (2008) 3247–3258, http://dx.doi.org/10.1093/jxb/ern176
[57] L.Y. Tang, W. Sakamoto, Tissue-specific organelle DNA degradation mediated by DPD1 exonuclease, Plant Signal. Behav. 6 (2011) 1391–1393, http://dx.doi.org/10.4161/psb.6.9.16595
[58] E.P. Beers, Programmed cell death during plant growth and development, Cell Death Differ. 4 (1997) 649–661, http://dx.doi.org/10.1038/sj.cdd.4400297
[59] J.T. Greenberg, Programmed cell death: a way of life for plants, Proc. Natl. Acad. Sci. U.S.A. 93 (1996) 12094–12097, http://dx.doi.org/10.1073/pnas.93.22.12094
[60] B. Kolano, M. Dorota, Siwinska, Jolanta, Endopolyploidy patterns during development of *Chenopodium quinoa*, Acta Biol. Cracoviensia Ser. Bot. 51 (2009) 85–92.
[61] N. Kudo, Y. Kimura, Flow cytometric evidence for endopolyploidization in cabbage (*Brassica oleracea* L.) flowers, Sex Plant Reprod. 13 (2001) 279–283, http://dx.doi.org/10.1007/s004970100066.